Room Temperature, Intrinsic Vacancy Mediated Ferromagnetism in Cr:Ga_2Se_3 /Si

E. N. Yitamben,[1,*] T. C. Lovejoy,[1] A. B. Pakhomov,[2] S. M. Heald,[3] F. S. Ohuchi,[2] and M. A. Olmstead[1]

[1] *University of Washington, Department of Physics, Box 351560, Seattle, Washington 98195, USA*
[2] *University of Washington, Department of Materials Science and Engineering, Box 352120, Seattle, Washington 98195, USA*
[3] *Advanced Photon Source, Argonne National Laboratory, Argonne, Illinois 60439, USA*

(Dated: January 12, 2010)

Room temperature ferromagnetism is reported in laminar, epitaxial, semiconducting films of Cr-doped Ga_2Se_3 on Si(001), with a room temperature saturation moment of 4 μ_B/Cr. The intrinsic-vacancy structure of defected-zinc-blende $\beta-Ga_2Se_3$ enables Cr incorporation in a locally octahedral site without disrupting long-range order, determined by x-ray absorption spectroscopy, as well as strong overlap between Cr 3*d* states and the Se 4*p* states lining the intrinsic vacancy rows, observed with photoemission. A mechanism is proposed whereby ordered intrinsic vacancies mediate ferromagnetism.

PACS numbers: 68.35-p, 68.37.Ef, 75.50.Pp, 75.70.-i, 79.60.-i

Electrical spin injection into semiconductors is a major hurdle for implementation of semiconductor spintronic applications due to the large impedance mismatch between ferromagnetic (FM) metals and semiconductors. One solution is to employ a dilute magnetic semiconductor (DMS), with spin-polarized carriers, for the injector material; however, no material to date encompasses both room temperature ferromagnetism (RTFM) and silicon compatibility, two key components determining the practical value of a material for future spintronic applications. Spin injection into GaAs has been demonstrated from the FM-DMS Mn-doped GaAs.[1] However, the Curie temperature of Mn:GaAs is well below room temperature. High-Curie-temperature, wide-band-gap oxides and nitrides have attracted much interest since the original reports of room-temperature FM in transition-metal-doped TiO_2 and ZnO.[2,3] However, neither these nor other dilute wide-bandgap, room-temperature ferromagnetic (RTFM) materials have yet demonstrated clear spin polarization of carriers characteristic of true DMS, or been successfully integrated with Si, the leading candidate for spintronics due to its ubiquity, low spin-orbit interaction and long spin diffusion lengths. Moreover, the origin of ferromagnetism in dilute RTFM materials is still not well understood.

Spin polarization of carriers in a DMS naturally accompanies FM with a carrier-mediated mechanism of ferromagnetic ordering, as formulated for Mn:GaAs.[4] In recent models of defect mediation in dilute RTFM materials, ferromagnetic ordering is acquired only in the presence of structural defects, typically having open volume character, including vacancies, grain boundaries and surfaces,[5–10] which are difficult to control reproducibly. The intrinsic vacancy structure of Ga_2Se_3, where one-third of cation sub-lattice sites are vacant and the chalcogenide lone-pair states lining vacancy rows form anisotropic band-edge states,[11] is intermediate between band- and defect- mediated systems, making it a promising host for RTFM DMS with enhanced propensity both for RTFM and carrier spin polarization. Our demonstrated ability to fabricate ordered vacancy structures during epitaxial growth of Ga_2Se_3 on silicon[12] and to grow epitaxial TM-doped TiO_2 on Ga_2Se_3/Si[13] makes Ga_2Se_3 the natural choice for initial investigation.

RTFM has been demonstrated in many Cr-doped, wide-band-gap semiconductors, including TiO_2,[7] GaN,[14] AlN,[15] ZnTe,[16] and ZnO,[17] with Cr substituting on cation sites. Crystal-field splitting of the Cr d-states normally favors octahedral symmetry for 3^+ ($3d^3$), raising the question of whether low-concentration Cr will reside on tetrahedral substitutional sites (as in Cr:GaN[18]) or whether it will exploit the open structure of the Ga_2Se_3 lattice either to create a local octahedral environment or to occupy a vacancy and exhibit a different valence state.

This letter describes a new path to RTFM DMS through employing a host with intrinsic vacancies, demonstrated on Cr-doped Ga_2Se_3 grown epitaxially on Si(001). Cr:Ga_2Se_3 films have a room temperature saturation magnetic moment of $\sim 4\mu_B$/Cr. Photoemission and X-ray absorption measurements reveal that Cr^{3+} occupies an octahedral site without disrupting the long-range zinc-blende structure, likely due to Cr substitution for Ga, combined with a rotation of bonds around a single Se. Photoemission also shows the films remain semiconducting while the vacancy structure surrounding Se is significantly altered, as well as a strong overlap between the Se 4*p* states lining the vacancy rows and the occupied Cr 3*d* states.

Cr-doped Ga_2Se_3 films on As-terminated Si(001) substrates were prepared using molecular beam epitaxy in ultra high vacuum (UHV, base pressure 1×10^{-10} Torr). All samples were deposited at a substrate temperature $T_{sub} \approx 475 - 500$ °C, with a constant GaSe flux, with the only variation being the timing and amount of the Cr co-deposition. For the films discussed here, a buffer layer of pure Ga_2Se_3 was deposited before the co-deposition of GaSe and Cr. The buffer layer exposure measured by the quartz crystal monitor was 3.6 nm thick; XPS showed

1.2 − 1.5 nm film thickness. Previous work has shown that some As diffuses into the Ga_2Se_3 film, occupying Se sites.[19]

Magnetization (SQuID magnetometry) and Cr valence and local environment (X-ray absorption fine structure) were measured *ex situ* on 20 nm thick films (Figs. 1 and 2). Chemical composition, valence states and Cr multiplet structure were assessed on thinner films ($\sim 2-3$ nm) using beamline 7.0.1 at the Advanced Light Source (ALS) for *in-situ* high-resolution photoemission spectroscopy (Fig. 3) performed on graded concentration epitaxial layers of Cr-doped Ga_2Se_3 on Si(001) substrates to allow comparison of different Cr concentration films under identical growth conditions. These samples were grown by repeatedly moving a shutter across the Cr path to the sample during deposition, such that the final sample varied only in Cr concentration as a function of position on the sample.

Magnetic properties were measured *ex situ* using a Quantum Design MPMS-5S superconducting quantum interference device magnetometer (SQuID) to 10^{-7} emu sensitivity. Hysteresis measurements were conducted at 5 and 300 K. These films, grown as described earlier, were then taken to the Advanced Photon Source (APS) at Argonne National Laboratory (ANL) for *ex-situ* K-edge x-ray absorption near-edge spectroscopy (XANES) and extended x-ray absorption fine structure (EXAFS) at the PNC/XOR-CAT beamline 20BM. Samples were mounted on spinners and rotated about the sample normal at a few hertz, while linearly polarized x-rays near the plane of the sample hit the surface at grazing incidence, to minimize Bragg diffraction.

Previous work has shown films with low Cr concentration are laminar with a cubic microstructure similar to pure Ga_2Se_3 .[20] Above a solubility limit of about 8 atom % Cr in the incident flux, Cr-rich islands form and metallic states are observed.[20,21] No oxygen or oxide-component for Ga or Cr is found with *in situ* photoemission, but surface oxidation (up to $\sim$ 20% of cations) is observed upon atmospheric exposure.

Results. Narrow hysteresis loops at 5 K and 300 K of a Cr:Ga_2Se_3 film with 6 atom % Cr are shown in Fig. 1. The saturation moment per Cr atom at 300 K is $4 \pm 0.2\mu_B$, with an additional paramagnetic component below $\sim$ 10 K. The magnitude of the magnetic moment was independent of whether or not an additional As or pure Ga_2Se_3 capping layer was applied *in situ* to reduce surface oxidation upon atmospheric exposure, and scaled with Cr:Ga_2Se_3 film thickness within about 20%. Similar measurements on pure Ga_2Se_3 films showed no trace of ferromagnetism.

The local Cr structural environment was investigated with X-ray absorption spectroscopy at the Cr K-edge (Fig. 2). Comparison of the near-edge structure to relevant standards [Fig. 2(a)] indicates the line shape and edge energy are closest to those for CrSe, with a small oxide component apparent at higher energies (solid line is a linear combination of the CrSe (80%) and Cr_2O_3 (20%) standards). Surprisingly, no "pre-edge" peak is seen (c.f. Na_2CrO_4), indicating that Cr is not in a tetrahedral (non-centrosymmetric) local environment.

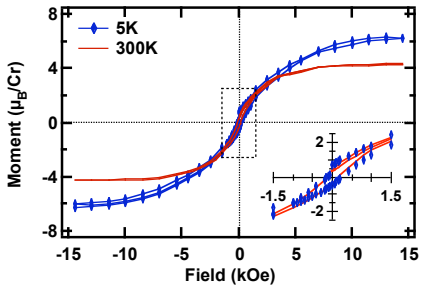

FIG. 1: (color online) Hysteresis loops at 5K and 300K of a 6% Cr-doped sample up to 1.5 T. The inset shows the region (box) near the origin.

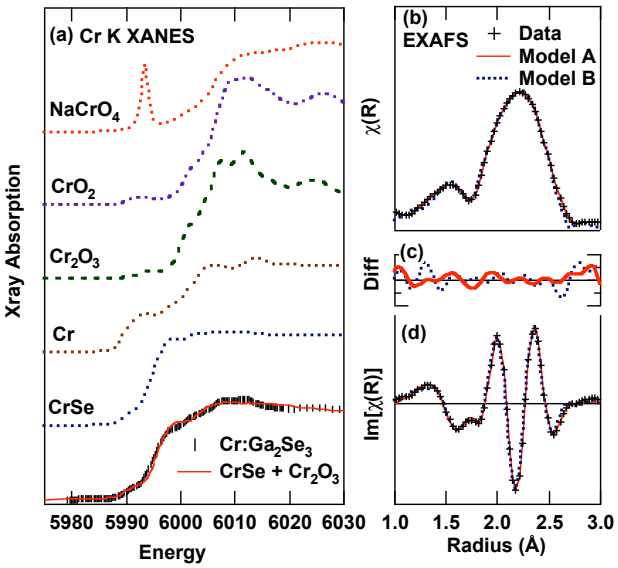

FIG. 2: (color online) Cr interaction within the crystal lattice probed using x-ray absorption fine structure: (a) Cr K-edge XANES spectra for for 6% Cr: Ga_2Se_3 as well as standards of CrSe, Cr metal, Cr_2O_3 , CrO_2 , and Na_2CrO_4; (b) k^2-weighted Fourier transform of Cr K-edge EXAFS data for 6% Cr:Ga_2Se_3 in crossed lines (+), with the fit to the data by FEFF calculations presented in solid and dotted lines comparing Model A and Model B; (c) Difference spectrum for Model A and Model B; (d) imaginary part of the k^2-weighted Cr K-edge EXAFS transform for 6% Cr:Ga_2Se_3 (+) and FEFF calculations for two models (lines).

The extended x-ray absorption fine structure (EXAFS) gives additional information about the local Cr environment. The data are not consistent with substitutional Cr_{Ga} or Cr_V, but rather fit well to six Se neighbors at a distance of $2.56 \pm 0.07\mathring{A}$. The fits shown in Fig. 2(b) are for the bulk compound $Cr_{0.8}Ga_{1.2}Se_3$ (dotted, model B) and the model shown in Fig. 4(d) (dashed, model

A), both including a surface oxide component with bond lengths of $2.0 - 2.1\AA$. The Ga K-edge (not shown) fits very well to pure Ga_2Se_3 , with about 20% in Ga_2O_3. The Ga-Se first nearest neighbor bond length is found to be $2.42 \pm 0.06\AA$, equal to that reported for EXAFS of bulk Ga_2Se_3 .[22]

Element-specific chemical environments and oxidation states were studied using photoemission spectroscopy over the composition range $0 - 6\%$ Cr. Throughout this range, the valence band maximum remains a few tenths of an eV below the Fermi level, indicating that the film remains a weakly-p-type semiconductor [Fig. 3(a)], and neither the valence band nor core-levels shift more than 0.1 eV. As the Cr concentration increases, a narrow band of Cr-related states is introduced at the top of the valence band [Fig. 3(a)], and the Se $3d$ environment is altered [Fig. 3(b)]. In pure Ga_2Se_3 , the Se peak exhibits two spin-orbit-split components, associated with Se adjacent to 1 (Se_{1V}) or 2 (Se_{2V}) vacancies.[12] As the Cr concentration increases, Se_{2V} decreases while the Se_{1V} increases. The Cr $2p$ emission [Fig. 3(c)] is characterized by a $2p_{3/2}$ multiplet structure similar to that in Cr_2O_3 ,[23] indicative of Cr 3^+ in an octahedral environment.

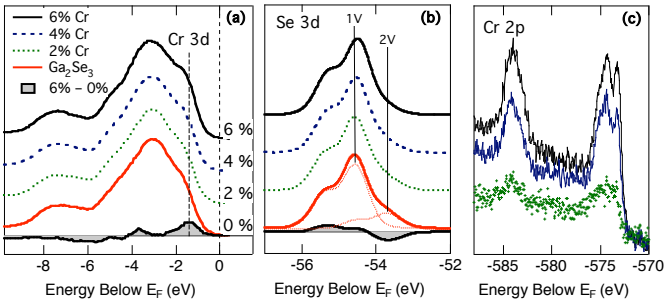

FIG. 3: (color online) Photoemission of $Cr:Ga_2Se_3$ as a function of Cr concentration in the incident flux (a) Valence band region, showing Cr $3d$ states increasing with Cr concentration; (b) Se $3d$, with fit to Se_{1V} and Se_{2V} shown for pure Ga_2Se_3 as dotted line ; (c) Cr $2p_{3/2}$ ($\sim$ 574 eV) and Cr $2p_{1/2}$ ($\sim$ 584 eV) emission, showing $2p_{3/2}$ multiplet structure (Ga_2Se_3 background subtracted). The shaded curves highlight the difference between 6% Cr and pure Ga_2Se_3 .

Discussion. The measured room-temperature moment of 4 ± 0.2 μ_B per Cr indicates the vast majority of Cr atoms are magnetically active, and is consistent with Cr 2^+ (4 μ_B/Cr) or Cr 3^+ (3 μ_B/Cr), but not Cr 4^+ (2 μ_B/Cr). The only potential ferromagnetic impurity phase is CrO_2, since Cr, CrSe,[24] Cr_2O_3,[25] CrGa,[26] and CrAs[27] are antiferromagnetic (although zincblende CrSe is theoretically predicted to be a ferromagnetic half-metal,[28] and zincblende CrAs is half-metallic and RTFM[29,30]) and $CrSi_2$ is diamagnetic,[31] but Cr_2O_3 is far more likely to occur than CrO_2 under our experimental conditions. Also, the Cr K-edge spectra indicate oxide bond lengths 10% longer than those of CrO_2, but consistent with Cr_2O_3, and an oxide fraction too small to account for the measured signal. Even though the magnetic moment in our films is more consistent with that of Cr 2^+, the valence band alignment and the model (discussed below) indicate that the prominent valence here is Cr 3^+ with the additional magnetic moment arising from some combination of surface enhancement, spin-orbit coupling, and/or impurity band exchange.

The absence of a pre-edge peak in Cr K-edge spectrum demonstrates that Cr does not substitute on a tetrahedral Ga or vacancy site, as it does in Cr:GaN[18] or Cr:ZnTe,[32] and the energy of the edge is consistent with a formal valence of Cr 2^+ (as in CrSe) and/or Cr 3^+(with Se neighbors screening more efficiently than oxygen). Both the Cr $2p$ multiplet structure and the maintenance of semiconducting band structure up to 6% Cr indicate that electronically Cr 3^+ is replacing Ga 3^+. At higher concentrations, where we also observe formation of Cr-rich islands, photoemission shows both metallic states at the Fermi level and a different Cr $2p$ lineshape.[21]

In bulk $(Ga,Cr)_2Se_3$ compounds, Cr is in an octahedral environment while Ga is in a tetrahedral environment.[33–36] In a perfect zincblende lattice, there is no locally octahedral site: the octahedral holes of the anion sublattice are tetrahedral holes in the cation sublattice, and vice versa. In Ga_2Se_3 , however, one third of the Se-sublattice octahedral holes are adjacent to two Ga atoms and two vacancies [Fig. 4(a)]. If Cr replaces one of these Ga atoms [Fig. 4(b)], the isoelectronic Cr3+ can obtain its preferred octahedral environment by shifting to the Se octahedral hole [Fig. 4(c)] while the only remaining adjacent Ga shifts to a neighboring vacant cation site [Fig. 4(d)]. This simple rotation around a single Se atom changes the nature of 3 vacancies (1 filled by the shifted Ga and 2 now adjacent to Cr) and leaves the Se sublattice intact. A fit of our EXAFS data to this model [Fig. 2(b), dashed (model A)] finds a nearest-neighbor bond length of $2.55 \pm 0.07\AA$, indicating the Se atoms contract locally towards the Cr from their ideal positions $2.70\AA$ away, and is a slightly better fit to the data than was the $Cr_{0.8}Ga_{1.2}Se_3$ structure (model B). The altered vacancy structure explains both the Se $3d$ and STM data, as well as the solubility limit of about 1 Cr per $3 - 4$ intrinsic vacancies.

Our initial choice of the material for the new type of DMS was based on compatibility with silicon and empirical considerations regarding the role of defects in dilute RTFM wide-bandgap materials. With the information on the electronic bands and structure of $Cr:Ga_2Se_3$ described above, we can now discuss a possible origin of FM ordering in this material. A semi-quantitative polaronic model proposed by Coey and collaborators[5] is frequently invoked in discussions of RTFM mechanisms in oxides. While the original model was formulated for n-type oxides, where donors are associated with oxygen vacancies, we can adopt it for the p-type case, as both the defect states (acceptors) and the magnetic impurity states in $Cr:Ga_2Se_3$ are located close to the valence band maximum. The geometric conditions of ferromagnetism (magnetic impurity concentration below the

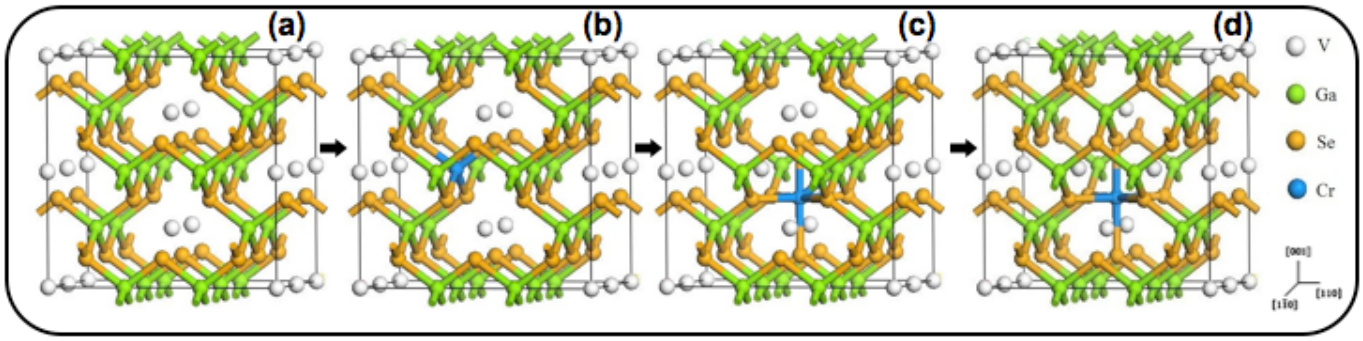

FIG. 4: (color online) Crystal model: (a) Ga_2Se_3 supercell; (b) Cr replaces a Ga in the Ga_2Se_3 structure; (c) Cr moves to an octahedral site, leaving the previous site vacant; thus (d) causing a Ga to move to a previously vacant site.

percolation threshold, and magnetic polaron concentration above percolation)[5] are clearly satisfied in our films. To obtain high Curie temperature, a high degree of hybridization of the Cr *d*-states with the defect states (acceptors in our case) is required; this condition is also satisfied in Cr:Ga_2Se_3. The Cr-induced states at the top of the valence band [Fig. 3(a)] overlap the Se lone-pair states lining the vacancy rows, suggesting strong hybridization between the Cr t_{2g} and Se *s,p* states. In this *p*-type material, long-range conduction is expected along the vacancy rows, although these bands are disrupted by the Cr-induced defects. This suggests a model similar to that proposed by Coey et al.[5] for indirect exchange, which will also result in spin polarization of carriers.

In conclusion, Cr-doped Ga_2Se_3 is shown to be a room temperature ferromagnet compatible with silicon, and we anticipate the high quality epitaxial interface will promote spin-preserving transport. The intrinsic vacancies enable Cr to find an octahedral local environment, and exhibits strong overlap between Cr *d*-states and Se states lining the vacancy rows that likely mediates the ferromagnetic interaction.

Acknowledgments

This work is supported by the NSF Grant DMR 0605601. The authors: E.N.Y. further acknowledges support from the IBM Corporation, and T.C.L. from the IGERT through the University of Washington. The authors thank Eli Rotenberg, and Taisuke Ohta for all their discussions and suggestions. Photoemission experiments were performed at the ALS, at LBNL operated by the U.S. DOE under contract number DOE DE-AC02-05CH11231. Use of the APS at ANL is supported by the U.S. Department of Energy, Office of Science, Office of Basic Energy Sciences, under Contract DE-AC02-06CH11357.

* Electronic address: yitamben@u.washington.edu

[1] S. A. Wolf, D. D. Awschalom, R. A. Buhrman, J. M. Daughton, S. von Molnár, M. L. Roukes, A. Y. Chtchelkanova, and D. M. Treger, Science **294** (2001) 1488.
[2] Y. Matsumoto, M. Murakami, T. Shono, T. Hasegawa, T. Fukumura, M. Kawasaki, P. Ahmet, T. Chikyow, S. -Y. Koshihara, H. Koinuma, Science **291** (2001) 854-856.
[3] K. Ueda, H. Tabata, T. Kawai, Appl. Phys. Lett. **79** (2001) 988-990.
[4] T. Dietl, H. Ohno, F. Matsukura, J. Cibert, D. Ferrand, Science **287** (2000) 1019-1022.
[5] J. M. D. Coey, M. Venkatesan, C. B. Fitzgerald, Nature Mater. **4** (2005) 173-179.
[6] K. A. Griffin, A. B. Pakhomov, C. M. Wang, S. M. Heald, K. M. Krishnan, Phys. Rev. Lett. **94** (2005) 157204.
[7] T. C. Kaspar, S. M. Heald, C. M. Wang, J. D. Bryan, T. Droubay, V. Shutthanandan, S. Thevuthasan, D. E. McCready, D. R. Gamelin, A. J. Kellock, S. A. Chambers, Phys. Rev. Lett. **95** (2005) 217203.
[8] B. K. Roberts, A. B. Pakhomov, K. M. Krishnan, Appl. Phys. Lett. **92** (2008) 162511.
[9] A. Ney, K. Ollefs, S. Ye, T. Kammermeier, V. Ney, T. C. Kaspar, S. A. Chambers, F. Wilhelm, A. Rogalev, Phys. Rev. Lett. **100** (2008) 157201.
[10] G. Cohen, V. Fleurov, K. Kikoin, J. of Appl. Phys. **101** (2007) 09H106.
[11] M. Peressi, and A. Baldereschi, J. Appl. Phys. **83** (1998) 6.
[12] Taisuke Ohta, D. A. Schmidt, Shuang Meng, A. Klust, A. Bostwick, Q. Yu, M. A. Olmstead, F. S. Ohuchi, Phys. Rev. Lett. **94** (2005) 116102.
[13] D. A. Schmidt, T. Ohta, C. -Y. Lu, A. A. Bostwick, Q. Yu, E. Rotenberg, F. S. Ohuchi, M. A. Olmstead, Appl. Phys. Lett. **88** (2006) 181903.
[14] M. B. Haider, R. Yang, H. Al-Brithen, C. Constantin, D. C. Ingram, A. R. Smith, G. Caruntu, C. O'Connor, J. of Crystal Growth **285** (2005) 300.
[15] H. X. Liu, Stephen Y. Wu, R. K. Singh, Lin Gu, N. R. Dilley, L. Montes, M. B. Simmonds, Appl. Phys. Lett. **85**

(2004) 18.
[16] H. Saito, V. Zayets, S. Yamagata, K. Ando, Phys. Rev. Lett. **90** (2003) 207202.
[17] B. K. Roberts, A. B. Pakhomov, P. Voll, K. M. Krishnan, Appl. Phys. Lett. **92** (2008) 162511.
[18] J. J. Kim, H. Makino, M. Sakurai, D. C. Oh, T. Hanada, M. W. Cho, T. Yao, S. Emura, K. Kobayashi, J. Vac. Sci. Technol. B **23** (2005) 1308.
[19] T. Ohta, Ph.D. Dissertation, University of Washington (2004).
[20] E. N. Yitamben, T. C. Lovejoy, D. F. Paul, J. B. Callaghan, F. S. Ohuchi, M. A. Olmstead, Phys. Rev. B **80** (2009) 075314.
[21] E. N. Yitamben, T. C. Lovejoy, A. B. Pakhomov, S. M. Heald, F. S. Ohuchi, M. A. Olmstead, *in preparation.*
[22] S. Takatani, A. Nakano, K. Ogata, T. Kikawa, Jpn. J. Appl. Phys. **31** (1992) L458.
[23] S. A. Chambers, and T. Droubay, Phys. Rev. B **64** (2001) 075410.
[24] L. M. Corliss, N. Elliott, J. M. Hastings, R. L. Sass, Phys. Rev. **122** (1961) 5.
[25] M. Catti, G. Sandrone, G. Valerio, R. Dovesi, J. Phys. Chem. Solids **57** (1996) 11.
[26] O. Gourdon, S. L. Budko, D. Williams, G. J. Miller, Inorg. Chemistry **43** (2004) 3210.
[27] N. Kazama and H. Watanabe, J. of the Phys. Soc. of Jpn. **30** (1971) 1319-1329.
[28] Wen-Hui Xie, Ya-Qiong Xu, Bang-Gui Liu, D. G. Pettifor, Phys. Rev. Lett. **91** (2003) 3.
[29] H. Akinaga, T. Manago, M. Shirai, Jpn. J. of Appl. Phys. **39** (11B) (2000) L1118-L1120 (2000).
[30] J. F. Bi, J. H. Zhao, J. J. Deng, Y. H. Zheng, S. S. Li, X. G. Wu, Q. J. Jia, Appl. Phys. Lett. **88** (2006) 142509.
[31] Isao J. Ohsugi, Tsutomu Kojima, Isao A. Nishida, Phys. Rev. B **42** (1990) 16.
[32] M. Kobayashi, Y. Ishida, J. I. Hwang, G. S. Song, A. Fujimori, C. S. Yang, L. Lee, H-J. Lin, D. J. Huang, C. T. Chen, Y. Takeda, K. Terai, S-I. Fujimori, T. Okane, Y. Saitoh, H. Yamagami, K. Kobayashi, A. Tanaka, H. Saito, K. Ando, New J. of Phys. **10** (2008) 055011.
[33] I. Okonska-Kozłowska, K. Szamocka, E. Malicka, A. Waskowska, J. Heimann, T. Mydlarz, A. Gilewski, T. Gron, J. of Alloys and Compounds **366** (2004) 21.
[34] D. Skrzypek, I. Okonska-Kozłowska, K. Szamocka, E. Malicka, J. of Mag. and Mag. Mater. **285** (2005) 379.
[35] H. D. Lutz et al. M. Jung. Z. Anorg. Allg. Chem. **566** (1988) 55.
[36] A. A. Zhukov, Ya. A. Kesler, V. F. Meshcheryakov and A. V. Rozantsev, Sov. Phys. Solid State **25** (1983) 1328.